Spectral Energetics of the Canadian Climate Centre General Circulation Model

STEVEN J. LAMBERT

Canadian Climate Centre/CCRN, Downsview, Ontario, M3H 5T4, Canada

(Manuscript received 7 April 1986, in final form 12 December 1986)

ABSTRACT

The available potential energy–kinetic energy budget of the Canadian Climate Centre general circulation model for the months of January, April, July and October is presented in terms of the two-dimensional wavenumber. Five years of model results are compared to calculations based on observations taken during the First GARP Global Experiment (FGGE).

Qualitatively, the simulated budget is realistic but a few of the magnitudes of the energies and conversions between them are not well simulated, arising in part from an excess of zonal available potential energy and zonal kinetic energy caused by the model's polar regions being too cold.

1. Introduction

The generation, transformation and dissipation of energy are basic processes in the atmosphere. Probably the most common method of describing the atmospheric energy cycle is by use of the four-component system developed by Lorenz (1955). This scheme partitions atmospheric energy into zonal available potential energy (A_z), eddy available potential energy (A_e), zonal kinetic energy (K_z) and eddy kinetic energy (K_e) and describes the conversions taking place between these components. From the outset, obtaining reliable data has always been a problem in the study of atmospheric energetics and as a result, most studies have been confined to the Northern or extratropical Northern Hemisphere; e.g., Oort (1964) and Oort and Peixoto (1974). One of the first attempts to compute a global budget was made by Newell et al. (1974) who were able to obtain estimates of the four energies and most of the conversions.

In a generalization of Lorenz' approach, Saltzman (1957) proposed describing the energy cycle in terms of zonal wavenumber. In this representation, the A_e and the K_e of the Lorenz budget are decomposed into many components which permit the study of the energetics on a wide range of spatial scales. This approach has been used by many investigators to study the extratropical Northern Hemisphere and a compilation of results was given in Saltzman (1970). Kanamitsu et al. (1972) calculated the zonal wavenumber budget for the tropics, and Price (1975) computed the available potential energy (APE) and the kinetic energy (KE) spectra for the Southern Hemisphere but he did not compute any of the conversion terms. Since Saltzman's representation is more complex than that of Lorenz, the data problem is even more acute and further application of this technique also awaited the availability of high quality global data.

Baer (1972) described an alternate scale dependent method of representing atmospheric energy based on the degree of the associated Legendre polynomials. Burrows (1976) studied the KE of the Northern Hemisphere by employing a budget based on this two-dimensional wavenumber. Unfortunately, further application of this approach was also hindered by the lack of suitable observational data.

The lack of high quality data was remedied somewhat during the Global Weather Experiment (FGGE). For the first time, global spectral energetics could be computed with some degree of confidence. Kung and Tanaka (1983) presented global Lorenz and Saltzman budgets for the two special FGGE observing periods, and Lambert (1984, hereafter L84) formulated an APE–KE budget in terms of the two-dimensional wavenumber and gave results for the four midseason months of the FGGE year.

Although the FGGE exercise yielded datasets of high quality, the results of Kung and Tanaka suggest that data problems remain. Using two independently analyzed datasets, one produced by the European Centre for Medium Range Weather Forecasts (ECMWF) and the other by the Geophysical Fluid Dynamics Laboratory (GFDL), they were able to compute two values for each budget quantity. A comparison of like quantities showed reasonable agreement except for the A_z to K_z, and A_e to K_e and the K_e to K_z conversions, some of which differed by more than 100 percent. Since the APE to KE conversions depend strongly on the vertical motion, it is not surprising that such large differences occur in these terms, but it is somewhat disturbing that large differences occur in the K_e to K_z conversion.

Many values of the Lorenz budget terms for flows

simulated by general circulation models (GCM) have appeared in the literature. These generally appear as Northern Hemisphere results only, or as separate budgets for the Northern and Southern Hemispheres with only the Northern Hemisphere compared to observations. Spectral investigations of model simulations for the Northern Hemisphere have been presented by Tenenbaum (1976, 1982) and Baker et al. (1977) and for both hemispheres and the tropics by Otto-Bliesner (1984). In general, GCMs qualitatively simulate the observed energy cycles but are less successful in reproducing the magnitudes of the energies of the components and the magnitudes of the conversions between them.

The present study will give the spectral energetics of the Canadian Climate Centre (CCC) GCM. In order to place its energetics in a more familiar light, the Lorenz budgets of several models, including the CCC, and the Lorenz budgets based on observational data are presented for the solsticial seasons. This is followed by the CCC GCM's energetics in the form of a global vertically integrated APE–KE budget in terms of the two-dimensional wavenumber. The budget results are computed for the four midseason months of a five year simulation and are compared to budget results based on observations taken during the FGGE year.

2. Model

The formulation of the CCC GCM is described in Boer et al. (1984a). It is a global sigma-coordinate spectral model with a triangular truncation at 20 waves and has ten levels with the uppermost at $\sigma = 0.01$ (10 mb). The climatology of the model is given and is compared to observations in Boer et al. (1984b). For the present study, the model was run for five years in an annual cycle mode and its output was sampled every 12 hours for each of the five January, April, July and October months.

It is necessary to transform the results from the model's sigma surfaces to pressure surfaces in order to do the energetics analysis. The spectral coefficients of vorticity and divergence on the sigma surfaces are transformed to Gaussian grid point values of the horizontal wind components on sigma surfaces. The point values are then interpolated to pressure surfaces. The vertical motion field, ω, is obtained diagnostically from the model's divergence field and is transformed to point values on pressure surfaces. In interpolating the wind components and the vertical motion fields, it is necessary to perform extrapolations above the model's uppermost sigma surface and below the model's $\sigma = 1$ surface, that is in regions where the interpolated pressure is greater than the surface pressure (p_s) or less than $0.01p_s$. This is done by assuming a zero lapse rate for all three fields. This procedure does not conserve mass in the regions of extrapolation. Temperature is obtained diagnostically from the geopotential using the hydrostatic equation and the two fields are interpolated to pressure. In order to extrapolate the temperatures below the model's $\sigma = 1$ surface, a lapse rate of 6.5×10^{-3} K m^{-1} is used, and the extrapolated geopotentials are made hydrostatically consistent with the extrapolated temperatures. The two fields are extrapolated independently above the model's uppermost sigma surface, resulting in small departures of the model output fields from hydrostatic consistency. After all the fields are available as Gaussian grids on pressure surfaces, they are transformed to spherical harmonic coefficients with the horizontal wind field being expressed as vorticity and divergence.

3. Analysis

The formulation of a spectral APE–KE budget is given in L84 in terms of the two-dimensional wavenumber or the degree of the associated Legendre polynomials. The following pair of equations is used to transform variables between the physical and the spectral domains:

$$x(\lambda, \phi) = \sum_{n=0}^{N} \sum_{m=-n}^{n} X_n^m P_n^m(\sin\phi) e^{im\lambda} \tag{1}$$

$$X_n^m = \frac{1}{2\pi} \int_0^{2\pi} \int_{-\pi/2}^{\pi/2} x(\lambda, \phi) P_n^m(\sin\phi) \cos\phi e^{-im\lambda} d\phi d\lambda \tag{2}$$

where P_n^m is the associated Legendre polynomial of the first kind of order m and degree n, X_n^m is a coefficient of the spherical harmonic representation of x, and N is the limiting wavenumber of the triangular truncation.

As was shown in L84, the global average of a quadratic quantity x^2, can be expressed in terms of spherical harmonic coefficients

$$\langle x^2 \rangle = \frac{1}{2} \sum_{n=0}^{N} \sum_{m=-n}^{n} X_n^m X_n^{*m} \tag{3}$$

where the asterisk denotes the complex conjugate. To obtain results in terms of the two-dimensional wavenumber, n, it is necessary to sum over m. Hence (3) becomes

$$\langle x^2 \rangle = \sum_{n=0}^{N} V(n)$$

where

$$V(n) = \frac{1}{2} \sum_{m=0}^{n} (2 - \delta_m{}^0)(X_n^m X_n^{*m}) \tag{4}$$

and δ is the Kronecker symbol. Equation (4) defines the two-dimensional wavenumber spectrum of $\langle x^2 \rangle$ in terms of spherical harmonic coefficients.

Following L84, the temporally averaged and vertically integrated APE–KE budget in terms of the two-dimensional wavenumber can be written as

TABLE 1. The Jan or Feb global Lorenz budget for several GCMs. The units of the zonal available potential energy (A_z), the eddy available potential energy (A_e), the zonal kinetic energy (K_z) and the eddy kinetic energy (K_e) are 10^4 J m^{-2}. The units of the A_z to A_e conversion, $C(A_z, A_e)$, the K_e to K_z conversion, $C(K_e, K_z)$, the A_z to K_z conversion, $C(A_z, K_z)$, and the A_e to K_e conversion, $C(A_e, K_e)$ are 10^{-2} W m^{-2}.

Model	A_z	K_z	A_e	K_e	$C(A_z, A_e)$	$C(K_e, K_z)$	$C(A_z, K_z)$	$C(A_e, K_e)$
CCC Jan	506	102	71	69	278	46	13	259
OSU Jan from Schlesinger–Gates (1980)	530	74	70	53	180	30	−70	—
NCAR Jan from Baker et al. (1977)	530	100	48	35	230	20	40	200
GISS Jan from Stone et al. (1977)	464	73	66	44	195	35	−44	240
GLAS Feb from Halem et al. (1978)	533	80	60	54	245	34	−61	310

$$\frac{\partial}{\partial t}A(n) = S(n) - C(n) + G(n) \tag{5}$$

$$\frac{\partial}{\partial t}K(n) = L(n) + C(n) + F(n) - D(n) \tag{6}$$

where $A(n)$ is the APE in wavenumber n, $S(n)$ is the nonlinear transfer of APE among waves, $C(n)$ is the conversion of APE to KE, $G(n)$ is the generation of APE, $K(n)$ is the KE in wavenumber n, $L(n)$ is the nonlinear transfer of KE among waves, $F(n)$ is the transfer of KE between adjacent waves by the Coriolis force, $D(n)$ is the dissipation of KE. The expressions used to compute the terms of (5) and (6) are contained in the Appendix.

The budget terms are computed for each of the four midseason months from a five-year simulation with a resolution of 20 waves. The APE to KE conversions are computed in terms of the vertical motion (ω) and the specific volume (α). Since it was not possible to compute the $G(n)$ and the $D(n)$ terms explicitly, they are computed as residuals.

4. Results

Before proceeding to the budget results in terms of the two-dimensional wavenumber, it is useful to compare the more conventional Lorenz budgets of several GCMs. Tables 1 and 2 give the vertically integrated results for those models for which global results are available. In each case, the vertical integration was done with a different uppermost data level as follows: CCC 10 mb, Oregon State University (OSU) 200 mb, National Center for Atmospheric Research (NCAR) 125 mb, Goddard Institute for Space Studies (GISS) 175 mb and Goddard Laboratory for Atmospheric Sciences (GLAS) 65 mb. This should not seriously affect most of the budget terms with the possible exception of A_z and K_z, which contain significant contributions from the stratosphere. In some cases, the global results are an average of the two hemispheric results which appear separately in the description of the model's energetics. Tables 3 and 4 present global budgets computed from a variety of observational sources for January (or the December to February season) and July (or the June to August season). Three of these were produced by the author from data for the FGGE year, one from observations for the period 1957–64 (Newell et al., 1974), one from observations for the period 1963–73 (Oort and Peixoto, 1983) and one by the author from operational objective analyses for the five-year period from 1979–83. The uppermost data level was 50 mb except 10 mb for the FGGE III-b results and 100 mb for the Newell et al. results.

Comparison of the models and the observations shows that the CCC GCM performs well and that its strength lies in its simulation of K_e and that its weakness lies in the simulation of A_z in July, K_z in January and the A_z to A_e conversions, all of which are somewhat too large. Also evident from the observations is the wide range of values in some of the budget results, e.g., the conversion of A_z to K_z. Consequently, it is difficult to assess model simulations of these terms.

Figure 1 displays the average amount of APE in each wavenumber, $A(n)$, for January, April, July and October for a five-year integration together with the results for the FGGE year. With only one year of observational data available for comparison, it must be assumed that the FGGE observations are representative of the atmosphere's two-dimensional wavenumber climate. The "error" bars on the GCM results extend two standard deviations of the five monthly means above and

TABLE 2. Same as Table 1 except for Jul or Aug.

Model	A_z	K_z	A_e	K_e	$C(A_z, A_e)$	$C(K_e, K_z)$	$C(A_z, K_z)$	$C(A_e, K_e)$
CCC Jul	542	104	58	61	234	39	44	259
OSU Jul	481	60	51	46	140	10	−20	—
NCAR Jul	420	69	36	27	200	0	50	210
GISS Jul	329	64	51	39	170	8	−95	195
GLAS Aug	448	76	58	57	227	26	−108	250

TABLE 3. The Lorenz budget from several observational sources for January (or Dec–Feb, DJF). The first three are for the year 1979 using the ECMWF Level III-b FGGE data, the GFDL Level III-b FGGE data and the NMC Level III-a FGGE data. The fourth (Newell et al., 1974) is from individual station data for the period 1956 to 1964, the fifth (Oort and Peixoto, 1983), is from station data for the period 1963–1973 and the sixth is from daily operational objective analyses of the NMC during the period 1979–83. The units are the same as those of Table 1.

Source	A_z	K_z	A_e	K_e	$C(A_z, A_e)$	$C(K_e, K_z)$	$C(A_z, K_z)$	$C(A_e, K_e)$
ECMWF FGGE III-b Jan	460	84	63	79	201	61	62	339
GFDL FGGE III-b Jan	488	86	62	80	230	38	324	390
NMC FGGE III-a Jan	469	76	72	78	189	34	—	—
Newell et al. (1974) DJF	400	51	71	72	160	30	2	—
Oort–Peixoto (1983) DJF	460	59	68	73	156	30	−2	220
NMC (1979–1983) Jan	477	82	62	78	202	41	—	—

below the five-year mean. Qualitatively, the model reproduces the $A(n)$ spectrum for each of the four months and its seasonal variation, but it is less successful in simulating the magnitudes of the $A(n)$ especially at small n. The results presented in Boer et al. (1984b) show that the upper tropospheres and stratospheres of both polar regions in the model are too cold, and this results in an excess of APE at small n and especially in the even wavenumbers which reflect the symmetry of the zonally averaged state about the equator.

Figure 2 displays the $S(n)$ term which describes the transfer of APE among waves. The GCM results show that the largest scales, wavenumbers one and two, lose energy in all four months and that wavenumbers seven and above gain energy by non-linear transfers. The wavenumbers in the band $3 \leqslant n \leqslant 6$ can either gain or lose energy depending on the season. Although this seasonal variation is rather subtle, it is evident in the FGGE observations. The preceding results show that the model performs well qualitatively, but as was the case for the $A(n)$ term, it has difficulty in simulating the magnitudes of the nonlinear transfers. In making the comparison between the model and the observations, it must be remembered that the $S(n)$ are dependent on the spectral resolution used in their calculation. Since the observations were computed with a resolution of 60 waves and the model with 20 waves, comparison of the GCM and the FGGE results at high wavenumbers is inappropriate.

Figure 3 gives the APE to KE conversion terms, $C(n)$. In spite of the fact that this term is difficult to obtain from observations, the agreement between the model and FGGE is striking for all months except April. There is a great deal of structure in this term at small n and it undergoes considerable seasonal change. In general, its spectrum is characterized by a strong sharp maximum at low wavenumbers and a broad, less intense maximum at medium scales which are separated by a region of negative conversions. Most of the structure of this term at small n results from the zonal ($m = 0$) modes. The contributions from these modes to $C(n)$ are shown in Fig. 3. These zonal conversions arise from the mean meridional circulation, and are a combination of positive contributions from the direct Hadley circulation and negative contributions from the indirect Ferrel circulation.

The broad medium scale maximum occurring near $n = 10$ is the result of conversions taking place in synoptic-scale disturbances. With the exception of January, where the conversions are too weak, the model provides a good simulation of this part of the $C(n)$ spectrum.

Figure 4 gives the $K(n)$ spectrum. These results show that the KE is concentrated in the small wavenumbers and notably those with n odd. The concentration of energy in the odd modes arises because the $K(n)$ is expressed in terms of vorticity and divergence as given by (A3). The coefficients of the scaled zonal wind, $U = u\cos(\phi)/a$ can be expressed in terms of the vorticity and divergence as (Daley et al., 1976)

$$U_n^m = -\frac{\epsilon_n^m}{n}\zeta_{n-1}^m + \frac{\epsilon_{n+1}^m}{n+1}\zeta_{n+1}^m - i\frac{m}{n(n+1)}D_n^m. \quad (7)$$

For $m = 0$, the modes with n even will be symmetric about the equator and those with n odd antisymmetric.

TABLE 4. Same as Table 3 except for July (or Jun–Aug, JJA).

Source	A_z	K_z	A_e	K_e	$C(A_z, A_e)$	$C(K_e, K_z)$	$C(A_z, K_z)$	$C(A_e, K_e)$
ECMWF FGGE III-b Jul	380	93	36	60	138	52	61	347
GFDL FGGE III-b Jul	497	93	53	68	153	20	260	230
NMC FGGE III-a Jul	478	76	54	60	129	32	—	—
Newell et al. (1974) JJA	330	40	59	64	100	20	7	—
Oort–Peixoto (1983) JJA	400	49	55	64	99	21	11	170
NMC (1979–1983) Jul	426	76	46	62	131	41	—	—

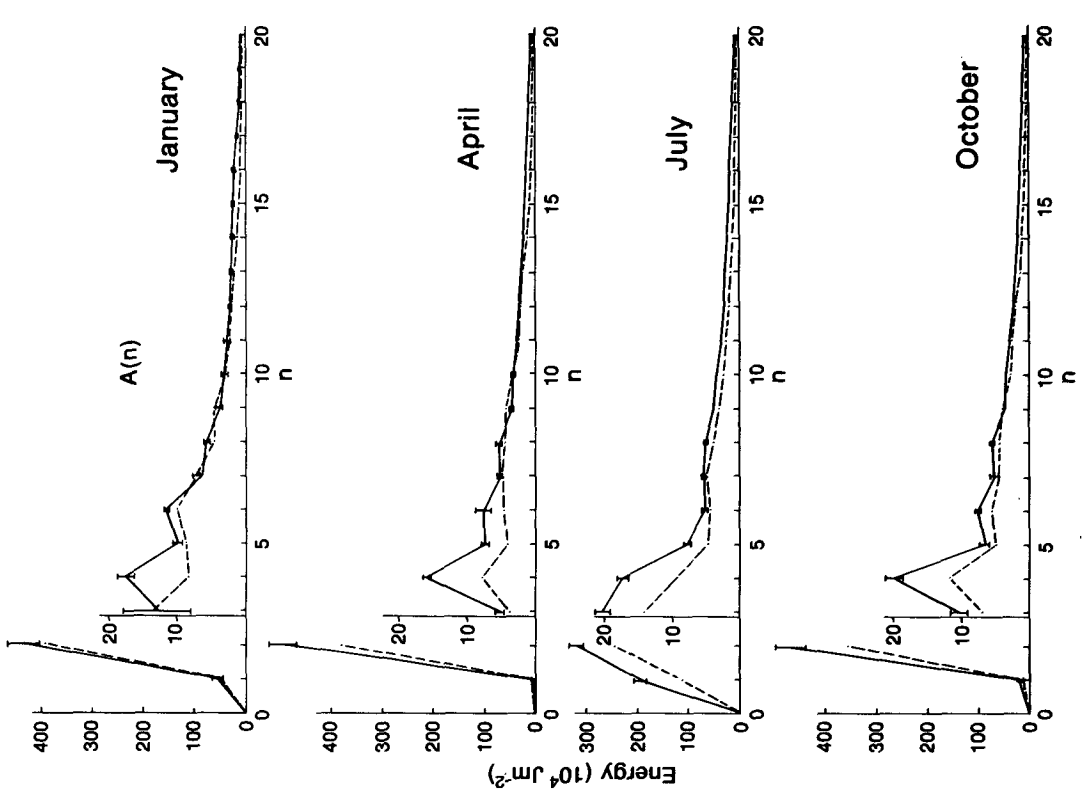

FIG. 1. The APE as a function of the two-dimensional wavenumber, $A(n)$. The solid line gives the January, April, July and October averages from a five-year simulation by the CCC GCM. The "error" bars extend two standard deviations of the five monthly means above and below the five-year mean. The dashed line gives the corresponding results from ECMWF analyses for the FGGE year. Note the change of scale between $n = 2$ and $n = 3$.

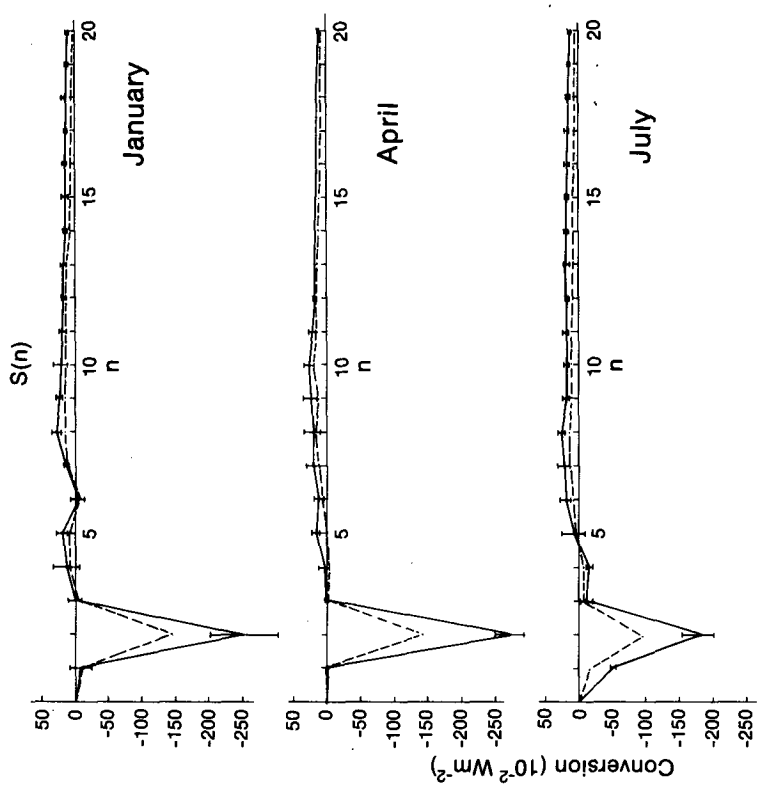

FIG. 2. As in Fig. 1 except for the APE nonlinear interaction term, $S(n)$.

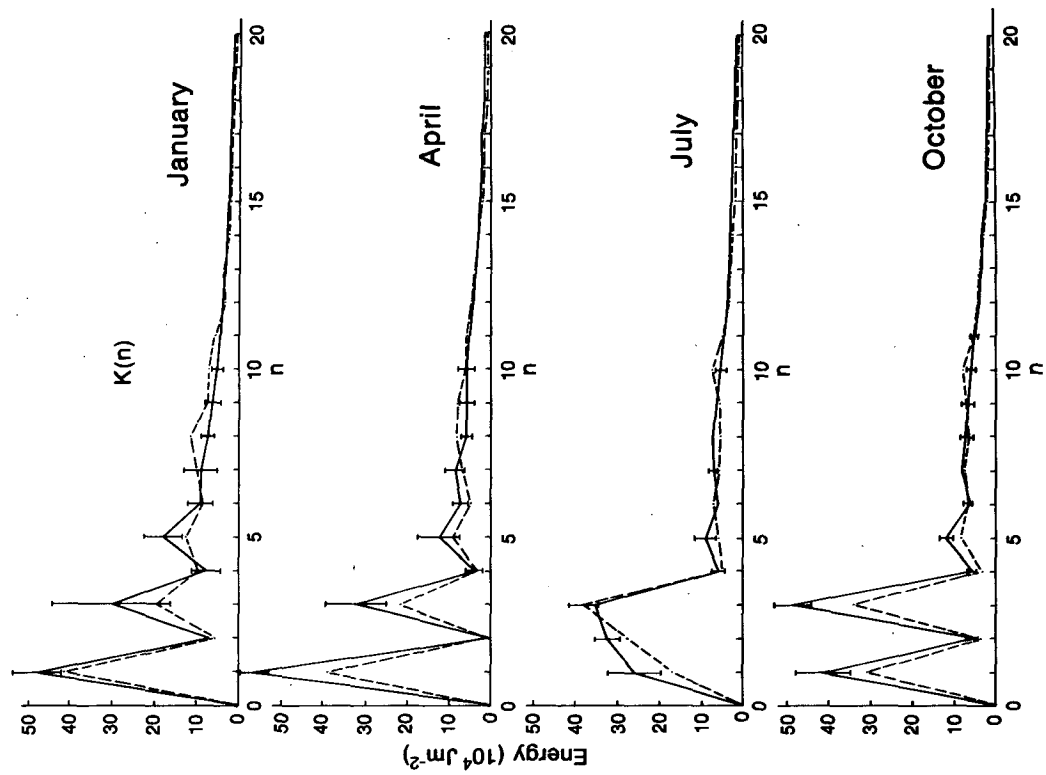

FIG. 4. As Fig. 1 except for the KE as a function of the two-dimensional wavenumber, $K(n)$.

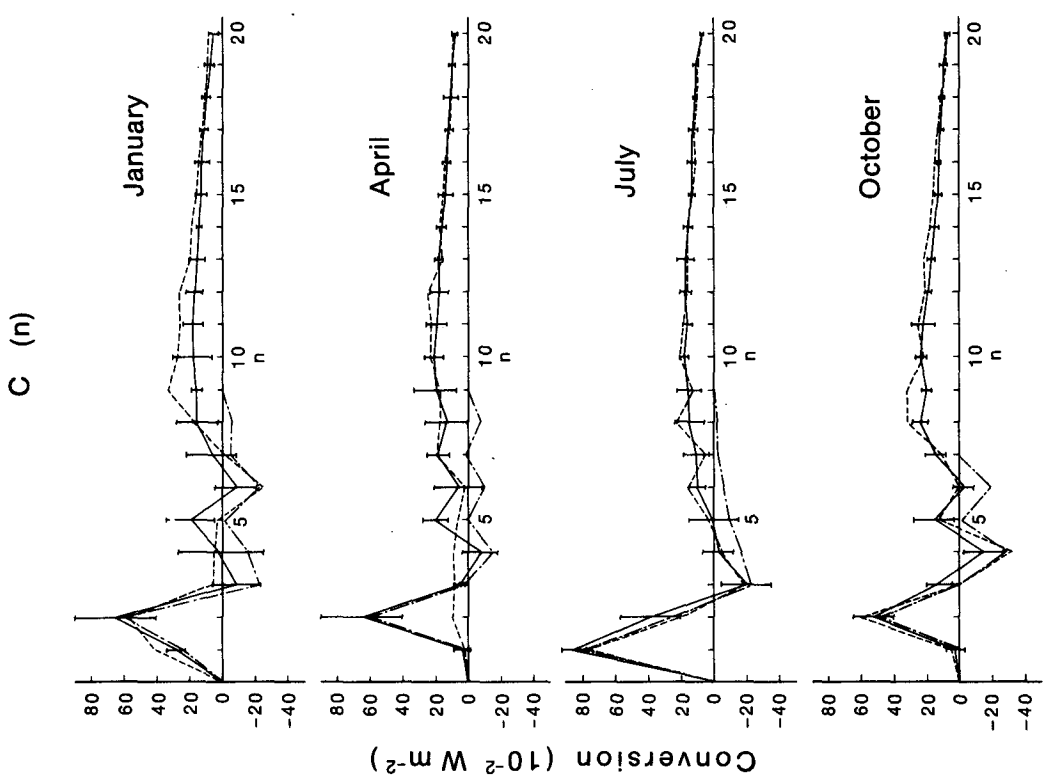

FIG. 3. As in Fig. 1 except for the APE to KE conversion term, $C(n)$. The alternating long and short dashed line displays the contributions from the zonal ($m = 0$) modes.

The above equation shows that for $m = 0$ the symmetric modes of the scaled velocity are expressed in terms of the antisymmetric modes of the vorticity. Since the scaling does not change the symmetry, the nearly symmetric zonal wind will produce large contributions in the odd modes of the $K(n)$.

The model results indicate that these modes contain too much energy which is a further result of the model's cold polar regions. Even though the model tends to have too much KE at small n values, it simulates the positions of the maxima and their relative strengths well, resulting in a good simulation of the seasonal variability.

Figure 5 displays $L(n)$ which is the transfer of KE to wavenumber n by nonlinear interactions among waves. The structure of the $L(n)$ term exhibits little seasonal change. Throughout the year this term is a source of energy for $n = 3$ and $n = 5$ and as a result, the nonlinear transfers are probably important in maintaining the large amounts of KE in these waves. Interestingly, the nonlinear interactions do not seem to be important in accounting for the large amount of energy in wavenumber one since $L(1)$ is, in general, a weak sink of energy. The KE in this wavenumber is maintained primarily by the APE–KE conversion term, $C(n)$, in January and July and by the Coriolis term, $F(n)$, in April and October. Comparison of model and observational results shows that the GCM has simulated the structure of the $L(n)$ for the small and medium n, except for a few instances in which the magnitudes are not satisfactory. For large n, the model and observations are not comparable because of the difference in the resolutions used in the calculations.

The $F(n)$ term is displayed in Fig. 6. This term arises in the two-dimensional budget as a result of the meridional structure of the Coriolis parameter. It describes exchanges of energy between adjacent wavenumbers and these exchanges take place such that rotational KE in wavenumber n is exchanged with divergent KE in wavenumbers $n + 1$ and $n - 1$ and divergent KE in wavenumber n is exchanged with rotational KE in wavenumbers $n + 1$ and $n - 1$. This term depends strongly on the divergence and as a result is difficult to obtain from observations. Both the model results and the observations show that this term is small for $n > 10$ and in the smaller n modes the model and FGGE agree rather well. At small n where the $C(n)$ term is a large source of energy, the $F(n)$ term is a sink and at slightly higher wavenumbers where the $C(n)$ is a sink of energy, the $F(n)$ is a source. Consequently, the $F(n)$ term is extracting energy from the large-scale direct circulation to provide the source of energy to drive the indirect circulation which is seen in the APE to KE conversions. The model appears to have performed well in simulating this term since the positions of the maxima and minima, the seasonal variation and the magnitudes agree with the FGGE results.

For completeness of the budget results, Table 5 displays the computation of the APE generation term, $G(n)$, and the KE dissipation term, $D(n)$, as residuals. These results show that $n = 1$ and especially $n = 2$ are the major sources of APE and most of the other wavenumbers are sinks. The dissipation, $D(n)$, tends to have its largest values in those wavenumbers where the KE is largest. There is, however, a negative value in January at $n = 2$. This value is the difference between two relatively large quantities and the negative value probably arises from errors introduced during the sigma to pressure interpolation referred in section 2. The $G(n)$ and $D(n)$ calculated from the model are not compared to observations because the uncertainties in the data render residual calculations unreliable.

5. Summary and conclusions

The simulation of the global APE–KE energy cycle by the CCC GCM has been presented in terms of the two-dimensional wavenumber and has been compared to the corresponding results from observations taken during the FGGE year. Qualitatively, the model and the observations are in good agreement. The main energy source in the budget is the generation of APE in wavenumber two. This energy, plus the energy generated in all other wavenumbers, is redistributed among all wavenumbers by nonlinear interactions as described by $S(n)$. The APE in each wavenumber is converted to KE in the same wavenumber as shown by the $C(n)$ term. At very small n, there is a relatively large direct conversion of APE to KE and at somewhat larger n, there is moderate indirect conversion of KE to APE. At medium scales ($n = 10$), there is a broad region of APE to KE conversions arising from synoptic-scale disturbances. The KE in each wavenumber is redistributed among other wavenumbers by nonlinear interactions as described by the $L(n)$ term. The KE is also exchanged between adjacent wavenumbers as shown by the Coriolis term, $F(n)$. In the larger scales, the action of this term is complementary to that of $C(n)$. At very small n, where the $C(n)$ is a large source, the $F(n)$ is a sink and at slightly larger n, where the $C(n)$ is a sink, the $F(n)$ term is the major source of energy for the indirect circulation. Finally, dissipation of KE as given by the $D(n)$ term occurs at all wavenumbers.

The model and observations disagree in the small n values of $A(n)$, $S(n)$ and $K(n)$, especially in those modes which have large contributions from A_z and K_z. Some of these differences arise from the fact that the model's polar regions are too cold, which results in an excess of A_z and K_z. It is encouraging to see the good agreement between the model and observations for the $C(n)$ and the $F(n)$ terms. Since these quantities depend strongly on the divergence and since the spectra of these terms have a great deal of structure, observational es-

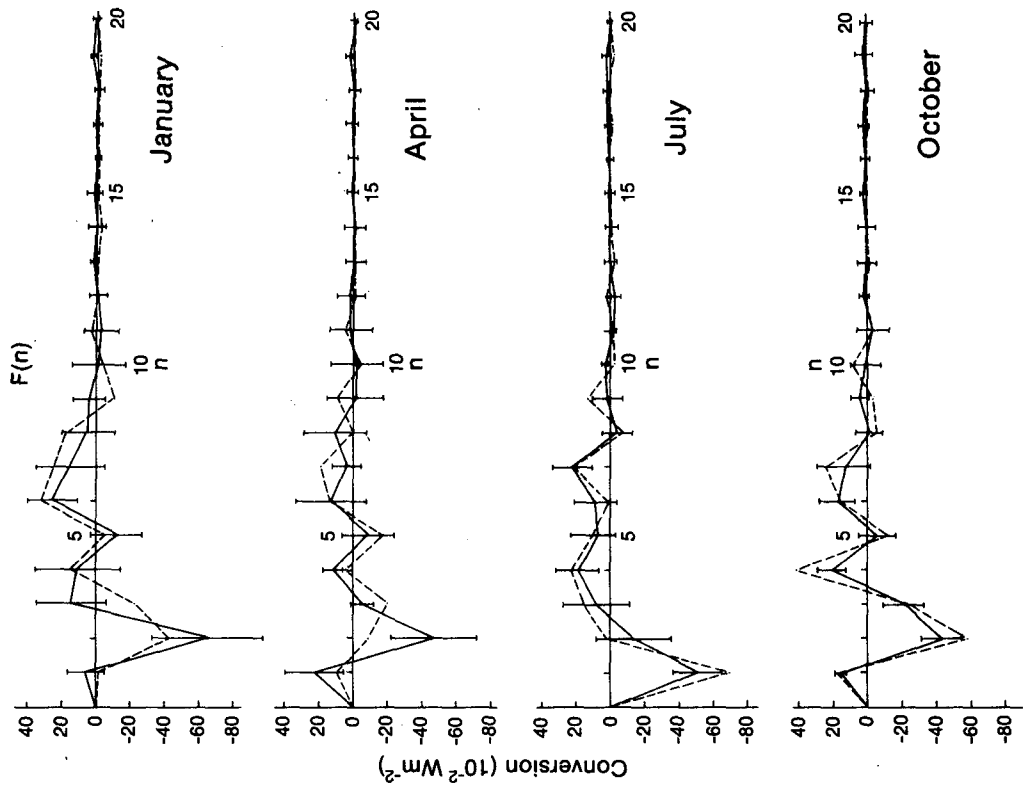

FIG. 6. As Fig. 1 except for the Coriolis term, $F(n)$.

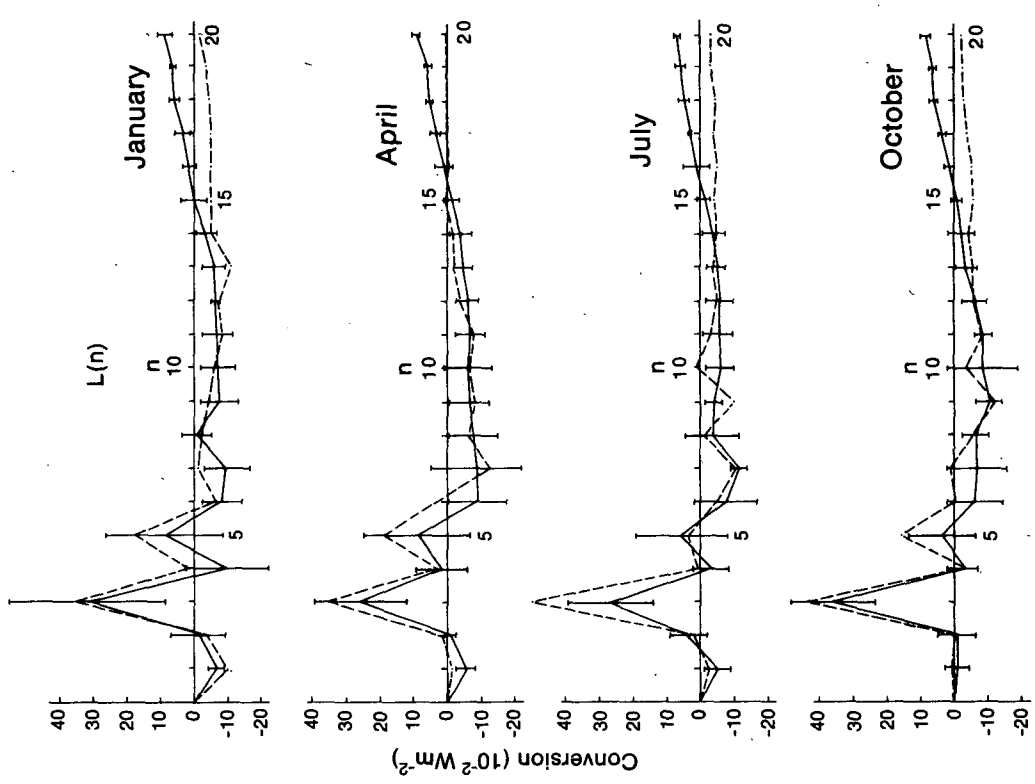

FIG. 5. As Fig. 1 except for the KE nonlinear interaction term, $L(n)$.

TABLE 5. The APE generation terms and the KE dissipation terms calculated as residuals. The units are 10^{-2} W m^{-2}.

	Generation				Dissipation			
n	Jan	Apr	Jul	Oct	Jan	Apr	Jul	Oct
1	37.1	3.4	146.0	5.0	27.3	19.8	30.3	17.6
2	328.4	344.6	244.4	308.5	−2.7	18.5	28.7	8.3
3	−9.1	3.0	−7.2	4.1	36.5	27.5	14.8	28.2
4	−7.2	−11.0	15.1	−3.8	3.5	4.5	12.5	2.4
5	1.8	3.4	−5.5	4.9	15.7	19.7	13.1	13.7
6	−5.6	−8.9	−6.1	13.1	9.1	7.8	11.7	6.9
7	−5.0	−0.5	−7.6	−1.4	12.5	13.1	21.4	20.5
8	−8.4	−6.7	−6.1	0.3	19.4	15.7	7.9	16.0
9	−4.2	−2.5	2.0	−1.7	12.2	11.5	13.6	12.6
10	−1.8	−2.2	3.8	0.1	9.7	13.6	15.3	15.5
11	0.4	−1.1	0.6	2.4	8.7	12.8	9.0	8.9
12	0.8	0.0	3.2	−0.1	9.6	12.7	9.5	12.1
13	−1.1	1.6	4.1	0.8	10.0	12.4	13.5	12.8
14	−0.9	−0.9	0.4	0.1	10.2	12.3	12.1	11.9
15	−3.1	−1.3	−0.8	−0.6	13.4	13.2	12.6	12.5
16	−3.3	−3.0	−1.8	−2.1	13.0	13.0	13.9	14.0
17	−2.8	−2.7	−2.4	−2.5	15.1	16.6	15.6	14.7
18	−5.2	−4.1	−2.9	−3.8	15.1	15.0	16.5	15.5
19	−5.1	−3.5	−1.8	−3.6	16.9	17.7	17.2	17.1
20	−4.0	−2.9	−2.7	−2.8	15.6	13.8	13.9	14.0

timates of these quantities are open to question. The agreement with observations implies a degree of confidence in both the model simulations and the estimates from observations.

As a result of the sigma-to-pressure coordinate transformation, the computed budget terms are subject to errors whose magnitudes are difficult to estimate. This difficulty is compounded in this study because the generation and dissipation terms are obtained as residuals. Clearly, an improvement to this or other studies of model energetics would be to compute the generation and dissipation terms explicitly to aid in assessing the reliability of the budget calculations.

Acknowledgments. The author gratefully acknowledges the efforts of Lynda Smith, who typed the manuscript.

APPENDIX

The following expressions were used to compute the budget terms of (5) and (6). The symbols have their usual meaning and the integration with respect to M represents a temporal average over the mass of the atmosphere. The details of the derivations can be found in L84. The APE of wavenumber n, $A(n)$, is

$$A(n)=\frac{1}{4}\int_M \sum_{m=0}^{n} C_p\gamma(2-\delta_m{}^0)(T_n{}^{+m}T_n^{*+m})dM \quad \text{(A1)}$$

The transfer of APE to wavenumber n by nonlinear interaction, $S(n)$, is

$$S(n)=\frac{1}{4}\int_M \sum_{m=0}^{n} C_p\gamma(2-\delta_m{}^0)(T_n{}^{+m}R_n^{*m}T_n^{*+m}R_n{}^m)dM \quad \text{(A2)}$$

where γ is the static stability, δ is the Kronecker symbol and

$$R_n{}^m=\left\{-\frac{u}{a\cos\phi}\frac{\partial T}{\partial\lambda}-\frac{v}{a}\frac{\partial T}{\partial\phi}-\omega\left(\frac{\partial T}{\partial p}-\frac{R}{pC_p}T\right)\right\}_n^m$$

where

$$\{(\ )\}_n{}^m=\frac{1}{2\pi}\int_{-\pi/2}^{\pi/2}\int_0^{2\pi}(\ )P_n{}^m\cos\phi e^{-im\lambda}d\lambda d\phi.$$

The KE in wavenumber n, $K(n)$, is

$$K(n)=\frac{1}{4}\int_M \sum_{m=0}^{n}(2-\delta_m{}^0)\times\frac{a^2}{n(n+1)}(D_n{}^mD_n^{*m}+\zeta_n^{*m}\zeta_n{}^m)dM. \quad \text{(A3)}$$

The transfer of KE to wavenumber n by nonlinear interactions, $L(n)$, is

$$L(n)=\frac{1}{4}\int_M \sum_{m=0}^{n}(2-\delta_m{}^0)\frac{a^2}{n(n+1)}\times(D_n{}^mA_n^{*m}+D_n^{*m}A_n{}^m+\zeta_n{}^mB_n^{*m}+\zeta_n^{*m}B_n{}^m)dM \quad \text{(A4)}$$

where a is the radius of the earth, and

$$A_n{}^m=\left\{-\frac{u}{a\cos\phi}\frac{\partial D}{\partial\lambda}-\frac{v}{a}\frac{\partial D}{\partial\phi}-\omega\frac{\partial D}{\partial p}-D^2-\frac{1}{a^2\cos\phi}\frac{\partial}{\partial\phi}\times[(u^2+v^2)\sin\phi]-\frac{1}{a}\frac{\partial\omega}{\partial\phi}\frac{\partial v}{\partial p}-\frac{1}{a\cos\phi}\frac{\partial\omega}{\partial\lambda}\frac{\partial u}{\partial p}-\frac{2}{a^2\cos\phi}\left(\frac{\partial u}{\partial\phi}\frac{\partial v}{\partial\lambda}-\frac{\partial u}{\partial\lambda}\frac{\partial v}{\partial\phi}\right)\right\}_n^m$$

$$B_n^m = \left\{ -\frac{u}{a\cos\phi}\frac{\partial\zeta}{\partial\lambda} - \frac{v}{a}\frac{\partial\zeta}{\partial\phi} - \omega\frac{\partial\zeta}{\partial p} - D\zeta + \frac{1}{a}\frac{\partial\omega}{\partial\phi}\frac{\partial u}{\partial p} - \frac{1}{a\cos\phi}\frac{\partial\omega}{\partial\lambda}\frac{\partial v}{\partial p} \right\}_n^m .$$

The APE to KE conversion, $C(n)$, is

$$C(n) = \frac{1}{4}\int_M \sum_{m=0}^{n} \frac{R}{p}(2-\delta_m{}^0)(T_n^{*m}W_n{}^m + T_n{}^m W_n^{*m})dM \tag{A5}$$

The transfer of KE to wavenumber n by the Coriolis force, $F(n)$, is

$$F(n) = \frac{1}{4}\int_M \sum_{m=0}^{n} (2-\delta_m{}^0)\frac{a^2}{n(n+1)} \times (D_n{}^m E_n^{*m} + D_n^{*m}E_n{}^m + \zeta_n{}^m G_n^{*m} + \zeta_n^{*m}G_n{}^m)dM \tag{A6}$$

where

$$E_n{}^m = \{f\zeta - \beta u\}_n{}^m$$
$$G_n{}^m = -\{fD + \beta v\}_n{}^m.$$

The $F(n)$ term may be split into rotational and divergent parts:

$$F(n)^{\mathrm{ROT}} = -2\Omega a^2 \int_M \sum_{m=0}^{n} (2-\delta_m{}^0) \times \left[\frac{1}{n^2}\epsilon_n{}^m(\zeta_n^{*m}D_{n-1}^m + \zeta_n{}^m D_{n-1}^{*m}) + \frac{1}{(n+1)^2}\epsilon_{n+1}^m(\zeta_n^{*m}D_{m+1}^m + \zeta_n{}^m D_{n+1}^{*m}) \right] dM \tag{A7}$$

$$F(n)^{\mathrm{DIV}} = 2\Omega a^2 \int_M \sum_{m=0}^{n} (2-\delta_m{}^0) \times \left[\frac{1}{n^2}\epsilon_n{}^m(D_n^{*m}\zeta_{n-1}^m + D_n{}^m\zeta_{n-1}^{*m}) + \frac{1}{(n+1)^2}\epsilon_{n+1}^m(D_n^{*m}\zeta_{n+1}^m + D_n{}^m\zeta_{n+1}^{*m}) \right] dM \tag{A8}$$

where

$$\epsilon_n{}^m = \left(\frac{n^2-m^2}{4n^2-1}\right)^{1/2},$$

thus showing that this term describes rotational KE and divergent KE exchanges between adjacent wavenumbers.

REFERENCES

Baker, W. E., E. C. Kung and R. C. J. Somerville, 1977: Energetics diagnostics of the NCAR general circulation model. *Mon. Wea. Rev.*, **105**, 1384–1401.

Baer, F., 1972: An alternate scale representation of atmospheric energy spectra. *J. Atmos. Sci.*, **29**, 649–664.

Boer, G. J., N. A. McFarlane, R. Laprise, J. D. Henderson and J.-P. Blanchet, 1984a: The Canadian Climate Centre spectral atmospheric general circulation model. *Atmos.-Ocean*, **22**, 397–429.

——, —— and ——, 1984b: The climatology of the Canadian Climate Centre general circulation model as obtained from a five-year simulation. *Atmos.-Ocean*, **22**, 430–473.

Burrows, W., 1976: A diagnostic study of atmospheric spectral kinetic energies. *J. Atmos. Sci.*, **3**, 2308–2321.

Daley, R., C. Girard, J. Henderson and I. Simmonds, 1976: Short-term forecasting with a multilevel spectral primitive equation model. Part I—Model formulation. *Atmosphere*, **14**, 98–116.

Halem, M., J. Shukla, Y. Mintz, M. L. Wu, R. Godbole, G. Herman and Y. Sud, 1978: Comparisons of observed seasonal climate features with a winter and summer numerical simulation produced with the GLAS general circulation model. Rep. *JOC Study Conf. on Climate Models*, Washington, DC, GARP Publ. Ser., No. 22, Vol. 1, 207–253. [NTIS N8027917.]

Kanamitsu, M., T. Krishnamurty and C. Depradine, 1972: On scale interactions in the tropics during northern summer. *J. Atmos. Sci.*, **29**, 698–706.

Kung, E. C., and H. Tanaka, 1983: Energetics analysis of the global circulation during the special observation periods of FGGE. *J. Atmos. Sci.*, **40**, 2576–2592.

Lambert, S. J., 1984: A global available potential energy–kinetic energy budget in terms of the two-dimensional wavenumber for the FGGE year. *Atmos.-Ocean*, **22**, 265–282.

Lorenz, E. N., 1955: Available potential energy and the maintenance of the general circulation. *Tellus*, **7**, 157–167.

Newell, R. E., J. W. Kidson, D. G. Vincent and G. J. Boer, 1974: *The General Circulation of the Tropical Atmosphere, Vol. 2*, The MIT Press, 371 pp.

Oort, A. H., 1964: On estimates of the atmospheric energy cycle. *Mon. Wea. Rev.*, **92**, 483–493.

——, and J. P. Peixoto, 1974: The annual cycle of the energetics of the atmosphere on a planetary scale. *J. Geophys. Res.*, **79**, 2149–2159.

——, and ——, 1983: Global angular momentum and energy balance requirements from observations. *Advances in Geophysics*, Vol. 25, Academic Press, 355–490.

Otto-Bliesner, B., 1984: A global low-order spectral general circulation model. Part II: diagnosis of the seasonal energetics. *J. Atmos. Sci.*, **41**, 508–523.

Price, P. G., 1975: A comparison between available potential energy and kinetic energy estimates for the Southern and Northern hemispheres. *Tellus*, **27**, 443–452.

Saltzman, B., 1957: Equations governing the energetics of the larger scales of atmospheric turbulence in the domain of wave number. *J. Meteor.*, **14**, 513–523.

——, 1970: Large-scale atmospheric energetics in the wavenumber domain. *Rev. Geophys. Space Phys.*, **8**, 289–302.

Schlesinger, M. E., and W. L. Gates, 1980: The January and July performance of the OSU two-level atmospheric general circulation model. *J. Atmos. Sci.*, **37**, 1914–1943.

Stone, P. H., S. Chow and W. J. Quirk, 1977: The July climate and a comparison of the January and July climates simulated by the GISS general circulation model. *Mon. Wea. Rev.*, **105**, 170–194.

Tenenbaum, J., 1976: Spectral and spatial energetics of the GISS model atmosphere. *Mon. Wea. Rev.*, **104**, 15–30.

——, 1982: Integrated and spectral energetics studies of the GLAS general circulation model. *Mon. Wea. Rev.*, **110**, 962–980.